International Journal of Refractory Metals & Hard Materials 93 (2020) 105346

Contents lists available at ScienceDirect

International Journal of Refractory Metals & Hard Materials

journal homepage: www.elsevier.com/locate/IJRMHM

Improved mechanical properties of NbC-M2 high speed steel-based cemented carbide by addition of multi-walled carbon nanotubes

Reza Esmaeilzadeh[a,b], Cyrus Zamani[b,*], Hendrik Reinhardt[a], Michael Dasbach[a], Norbert Hampp[a], Amir Hadian[b], Ali Mohammad Hadian[b]

[a] Department of Chemistry, Philipps-University of Marburg, Hans-Meerwein Street, 35032 Marburg, Germany
[b] School of Metallurgy and Materials Engineering, College of Engineering, University of Tehran, Tehran, Iran

ARTICLE INFO

Keywords:
NbC
Cemented carbide
M2 high-speed steel
MWCNT
Hardness
Fracture resistance

ABSTRACT

Multi-walled Carbon Nanotubes (MWCNTs) are added to NbC-12 vol% M2 high-speed steel to investigate the effect on microstructural and mechanical properties. Powder mixtures containing small amounts of MWCNTs (0, 0.1, 0.3 and 0.9 wt%) were prepared and shaped into pellets using cold compaction. The green samples were sintered under high vacuum condition for 1 h at 1360 °C. In order to study the microstructure and phase evolution of the sintered cemented carbide, field-emission scanning electron microscopy (FESEM) equipped with energy-dispersive X-ray spectroscopy (EDS) and X-ray diffraction (XRD) analysis were used. Density was measured using Archimedes method and Vickers hardness was performed to characterize the mechanical properties including hardness and fracture resistance. Results show that addition of MWCNTs from 0 to 0.3 wt% significantly increases the hardness from 1101 ± 18 to 1470 ± 22 HV. However, higher MWCNTs content causes reduction in hardness value down to 997 ± 26 for 0.9 wt%. FESEM images and density measurement reveal better densification of the cemented carbide by adding MWCNTs up to 0.3 wt%. Further microstructural investigations on indented samples showed remarkable bridging mechanism activated by the presence of nanotubes in the sample containing 0.3 wt%. Despite the toughening effects of MWCNTs, the fracture resistance slightly improved and reached the maximum value of 3.55 ± 0.08 MPa.m$^{0.5}$ for NbC-M2–0.3 wt% MWCNTs. According to XRD phase analysis, no compositional changes were detected in samples containing MWCNTs.

1. Introduction

Cemented carbides are a class of materials featuring high hardness, relative good fracture resistance, and excellent wear properties that make them well-suited for cutting tools and wear-resistant materials [1]. In this family of materials, tungsten carbides cemented with cobalt (WC-Co), due to their desirable properties, have been used extensively on industrial scale [2]. However, during high-speed machining, the high temperature (~ 1000 °C) at the component/cutting tool edge leads to the partial transformation of WC to WO_3 [1,3]. The WO_3 starts to sublimate at high temperatures which causes loss in the tribo-oxidative wear [2,4]. Moreover, it is known that prolong contact with WC-Co causes health problems among workers [5–7]. On the other hand, recent studies show that niobium carbide (NbC) is a promising candidate to replace WC, especially under dry sliding conditions [4,8]. Contrary to WO_3, studies on the formation of niobium oxide (Nb_2O_5) under elevated working temperatures show that this is a non-toxic material and thermodynamically stable phase [4]. It should be mentioned that NbC has a density of 7.87 g/cm^3, which is about half the density of WC, thus enabling less mass consumption in a fixed volume.

Investigations on the NbC-based cemented carbides are mainly focused on the final properties of the cemented carbide using different metallic binders and sintering techniques [9–11]. A comprehensive review regarding the microstructure of cemented carbides can be found in the study by Garcia et al. [2]. Among various metallic binders, Fe-based metals seem to be cost-effective and environmentally friendly compared to the rivals [12–14]. In the research done by Hadian et al. [12], it is mentioned that adding alloying elements could enhance the wettability and bonding strength of NbC and Fe. They used 12 vol% of M48 high-speed steel (HSS) as the binder and fully dense cemented carbide bodies having a high hardness of about 15 GPa and low fracture resistance of about 1.6 MPa.m$^{0.5}$ were achieved by sintering at above 1300 °C. Comparing these values with the fracture resistance of NbC-Ni cemented carbides reported by Huang et al. [15–17], it is clear that further improvement in the fracture resistance is necessary for NbC-HSS cemented carbides in order to consider them as potential cutting tool

* Corresponding author.
E-mail address: c.zamani@ut.ac.ir (C. Zamani).

https://doi.org/10.1016/j.ijrmhm.2020.105346
Received 14 May 2020; Received in revised form 13 July 2020; Accepted 3 August 2020
Available online 09 August 2020

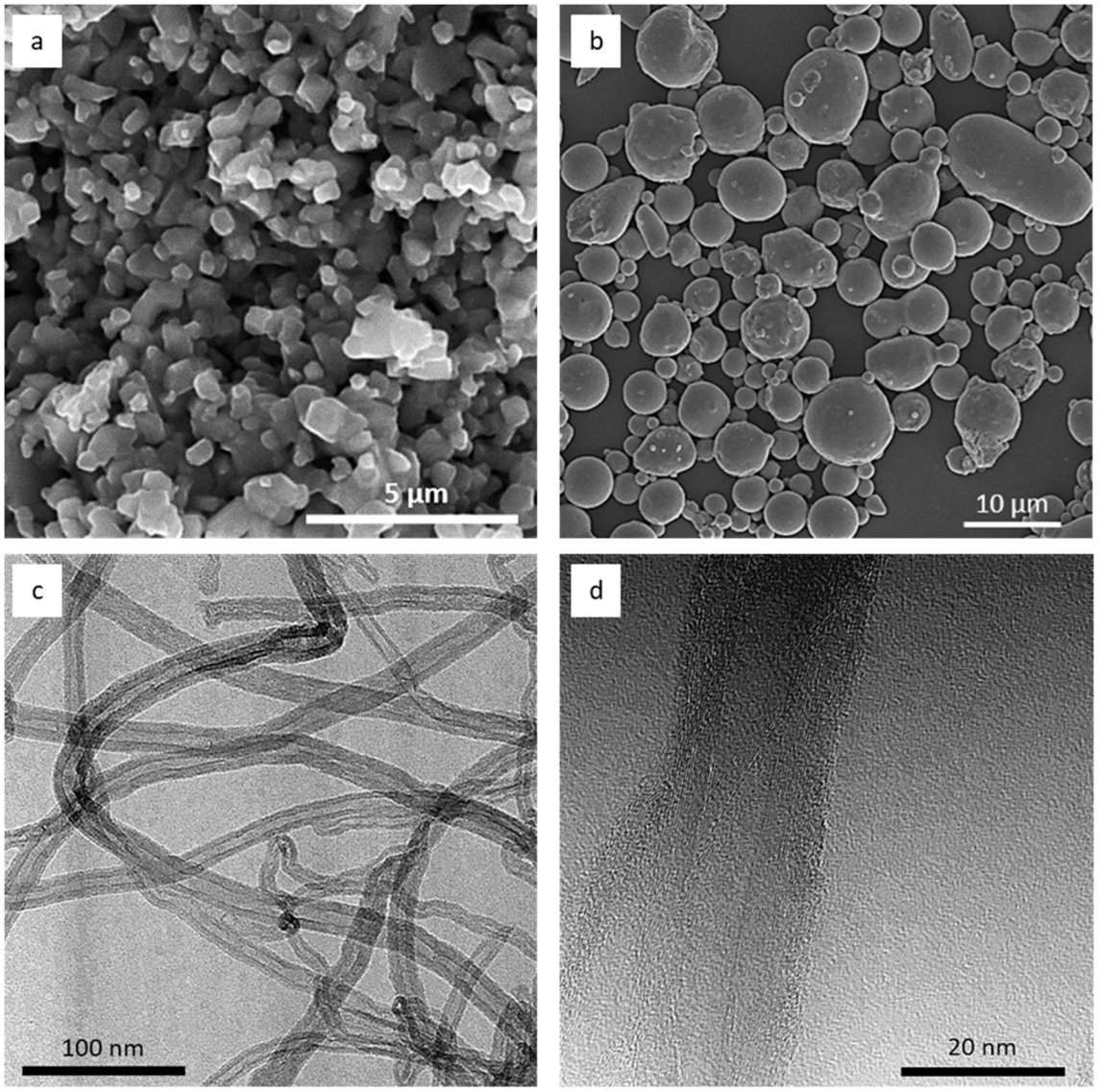

Fig. 1. SEM images of (a) NbC and (b) M2 high-speed steel as-received powders. (c) Bright-field TEM image, and (d) HRTEM image of original MWCNTs.

materials.

Among various materials, carbon nanotubes (CNTs), owing to their unique mechanical properties, are promising reinforcements in ceramic matrix composites (CMCs). Furthermore, CNTs exhibit thermal stability when they are exposed to high temperature processing of cemented carbides [18]. Addition of CNTs to CMCs has shown to improve physical and mechanical properties [18,19]. According to Xia et al. [19], magnificent toughening mechanisms such as bridging, pull-out, and/or crack branching are evident in CMCs containing CNTs. These mechanisms would reduce crack propagation and thus increase fracture resistance. Regarding WC-Co cemented carbide, incorporating CNTs into this matrix has already shown to attain significant improvement in hardness and fracture resistance [20]. Thus, considering the low fracture resistance of NbC-HSS cemented carbides, this study is aimed at incorporating CNTs into the NbC-based cemented carbides in order to obtain a better combination of hardness and fracture resistance. To the best of authors' knowledge, this approach has not been taken in NbC-based cemented carbides. Therefore, the effect of multi-walled carbon nanotubes (MWCNTs) on microstructure, hardness, and fracture resistance of NbC-M2 HSS cemented carbide is investigated here.

2. Materials and methods

2.1. Specimen fabrication

Powder technique was used for the fabrication of NbC-M2 cemented carbide based on the study by Hadian et al. [13]. First, commercially available NbC powder (MaTecK GmbH, 99 + %, Germany) was ball milled for 24 h in toluene with a ball to powder weight ratio (bpr) of 15 to break the agglomerates. Small amounts (i.e., 0, 0.1, 0.3, and 0.9 wt% of the total mixing mass) of MWCNTs (95 + %, OD: 8–15 nm, length: ~50 µm) were sonicated in toluene for 45 min. 12 vol% of M2 (5.5 W-4.5 Mo-3.75 Cr-1.75 V-0.8C- balance Fe), (16 µm-Sandvik Osprey, UK, 90%) high-speed steel as the metallic binder and 3 wt% paraffin wax as lubricant together with MWCNTs were added to the as-milled NbC powder. MWCNTs contents were chosen according to the study on WC-Co-MWCNTs [20]. In order to achieve well-dispersed mixtures, wet mixing was carried out for 6 h at a bpr of 5 using WC-Co balls. The mixed powders were dried using a rotary evaporator at 50 °C and 150 rpm. The dried mixtures were kept in an oven at 100 °C for 6 h to evaporate the remaining solvents prior to sintering. Powders were then shaped into small pellets with a diameter of 5.8 mm using a hydraulic press under a pressure of 200 MPa. For dewaxing (to remove paraffin),

samples were placed in a tube furnace and heated up to 300 °C for 12 h under a continuous flow of Ar + 5 vol% H_2 gas. Sintering was carried out under a high vacuum (~ 1.33×10^{-4} Pa) condition to prevent any oxidation reactions. Samples were heated up to 1360 °C at a heating rate of 400 °C/h, kept for 1 h, and then cooled down to room temperature inside the furnace.

2.2. Characterization

X-ray powder diffraction was employed using XRD apparatus (Ultima IV, Rigaku, Japan) with CuKα radiation to study the phase evolution of the as-received powders and the sintered samples. Field-emission scanning electron microscopy (FESEM) (JIB 4610F, JEOL, Japan) equipped with an EDS detector (XFlash 5010, Bruker, USA) was used to characterize the morphology and composition of the powders and sintered samples. The average grain size of NbC after sintering was measured based on the linear intercept method using an Image analyzer software (Digimizer, Version 5.4.4., MedCalc Software Ltd). In order to investigate the structure and morphology of MWCNTs, a small amount of nanotubes was dispersed on a copper grid for transmission electron microscopy (TEM) (LIBRA 200, Zeiss, Germany) study. The as-sintered samples were mechanically polished using grinding papers and diamond paste of 6 μm and 1 μm to achieve mirror-like polished surfaces. For density measurements, samples were immersed in water according to the Archimedes method (ASTM C373). Vickers hardness measurement was performed using 2 kgf at 10 s dwell time. For each sample, 5 indentation marks were taken to have more accurate results. Fracture resistance was calculated using the formula introduced by Shetty et al. [21] from the length of cracks induced by the indenter at the corners of indentation marks.

3. Results and discussion

3.1. Powder characterization

The morphology of the as-received powders is shown in Fig. 1. Based on the SEM image (Fig. 1(a)) NbC particles have irregular shapes with an average grain size of about 2 μm. The as-received NbC powder shows a high tendency for agglomeration which confirms the necessity of the initial ball milling step to break these agglomerates. The M2 HSS powder, however, has spherical shaped particles (Fig. 1(b)), which is associated with the production method (gas atomization). TEM images of the MWCNTs are presented in Fig. 1(c) and (d). The images elucidate the multi-walled structure and the high aspect ratio. With reference to Fig. 1(d), the wall spaces as well as the inner diameter were measured to be around 0.34 and 7.0 nm, respectively, while the outer diameter was different for different MWCNTs (depending on the number of layers). Due to Van der Waals forces and electrostatic attraction between nanotubes, a high tendency of agglomeration is found in MWCNTs [22,23]. Hence, an effective dispersion method is strongly required prior to processing. Sonication for 45 min was used in this study to disperse the MWCNTs effectively according to Lehman et al. [23].

3.2. Microstructural investigation

The microstructure of the sintered NbC-M2 containing different amounts of MWCNTs is shown in Fig. 2(a-d). All samples consist of two major phases: the light grey phase, which is NbC, and the dark grey phase, which is M2 HSS. There are some large porosities in the samples containing 0, 0.1, and 0.9 wt% MWCNTs, which are marked in Fig. 2(a), (b) and (d). Interestingly, an almost fully dense composite is achieved for the sample containing 0.3 wt% MWCNTs. The presence of large porosities is a sign of relatively low densities of the NbC-M2 cemented carbides. However, it is evident that by the addition of 0.3 wt% MWCNTs, the densification is enhanced, and the porosities disappear (Fig. 2(c)). During liquid phase sintering (LPS), especially under vacuum condition, carbon loss is usually observed [24], while an appropriate amount of carbon is essential for a good wettability and densification of the cemented carbides [1,3]. Adequate amount of carbon is required to reduce the residual surface oxides from the starting powders. Reduction of these oxides increases the surface energy between the carbide particles and metallic liquid phase resulting in improved wettability and higher consolidation. Therefore, it seems that the presence of carbon loss under high vacuum atmosphere hindered the full densification, despite the expected high densification of the NbC-M2 sintered at 1360 °C [13]. It should be pointed out that addition of MWCNTs as a carbon source compensated the carbon loss, thus improved the wettability and densification of the cemented carbides. As a result, it led to reduced porosities in the final microstructure. The high relative density (R.D.) (Table 1) for the sample containing 0.3 wt% MWCNTs compared to other samples confirms better densification of NbC-M2 HSS by adding MWCNTs. Enhanced densification of the WC-Co cemented carbide reinforced by MWCNTs is also reported by studies of Shi et al. [25] and Zhang et al. [20]. Moreover, the existence of large porosities in the sample containing 0.9 wt% is probably because of poor dispersion and clustering of MWCNTs.

The microstructural evolution can be observed in SEM micrographs taken at higher magnification, which are presented in Fig. 3. It is evident that NbC grain growth occurs by increasing the amount of MWCNTs (see Table 1 for grain size). Based on the existence of large interconnected faceted grains with round corners, it can be assumed that NbC grain growth is promoted by solution precipitation mechanism [26]. This mechanism takes place at the final steps of densification and could lead to lower fracture resistance properties [12]. The solution precipitation mechanism is more intense when the solubility of carbide in the molten binder increases [26]. Therefore, this microstructural feature certifies the better densification of NbC-M2 obtained by addition of MWCNTs. Similar carbide grain coarsening has already been reported in NbC-Ni [11] and WC-Co [27] cemented carbides as a result of carbon addition. Besides the two major phases (i.e., dark and grey) in the microstructure, a bright phase can be noted along the NbC grain boundaries (marked in Fig. 3(a)), which disappears when the amount of MWCNTs is increased (Fig. 3(a-d)). Based on the EDS analysis and previous reports by Hadian et al. [12], this phase is rich in W, Mo, and Cr elements. According to Huang et al. [11], the addition of carbon in NbC-based cemented carbides could change the solubility of elements in both binder and carbide phases. The more carbon dissolves into the binder, the less alloying elements exist in the metallic phase. Additionally, the excess carbon can also occupy the vacant octahedral positions of the NbC rock salt structure [28]. It is therefore proposed that by the addition of MWCNTs, the alloying elements depleted from the M2 binder and dissolved into the NbC structure to form mixed solid solution carbides.

Further microstructural examinations revealed the presence of another phase which was only observed in the sample containing 0.1 wt% MWCNTs as it is marked in Fig. 3(b). EDS analysis was conducted to reveal the elemental composition of this phase (Fig. 4 (a-g)). The selected area of the analysis is presented in Fig. 4(a). As expected, the EDS pattern illustrates the distribution of Nb and C mostly in the carbide and Fe in the binder phase. Moreover, the elemental maps reveal that at the right corner of Fig. 4(a), the light grey phase consists of Cr, Nb, and C, which suggests a mixed carbide is formed by the addition of 0.1 wt% MWCNTs. The formation of chromium carbides in steels is due to the reaction of chromium and carbon at high temperature (i.e., 800 °C) [28]. As a result, it is assumed that in the sample with 0.1 wt% MWCNTs, a large fraction of MWCNTs has dissolved into the M2 binder and led to the formation of this phase. Surprisingly, this phase was not detected for higher MWCNTs contents, which can be due to the lower solubility of alloying elements in the binder when MWCNTs are added. Furthermore, based on Fig. 4(f) and (g) even distribution of W and V can be observed in the microstructure which supports this explanation.

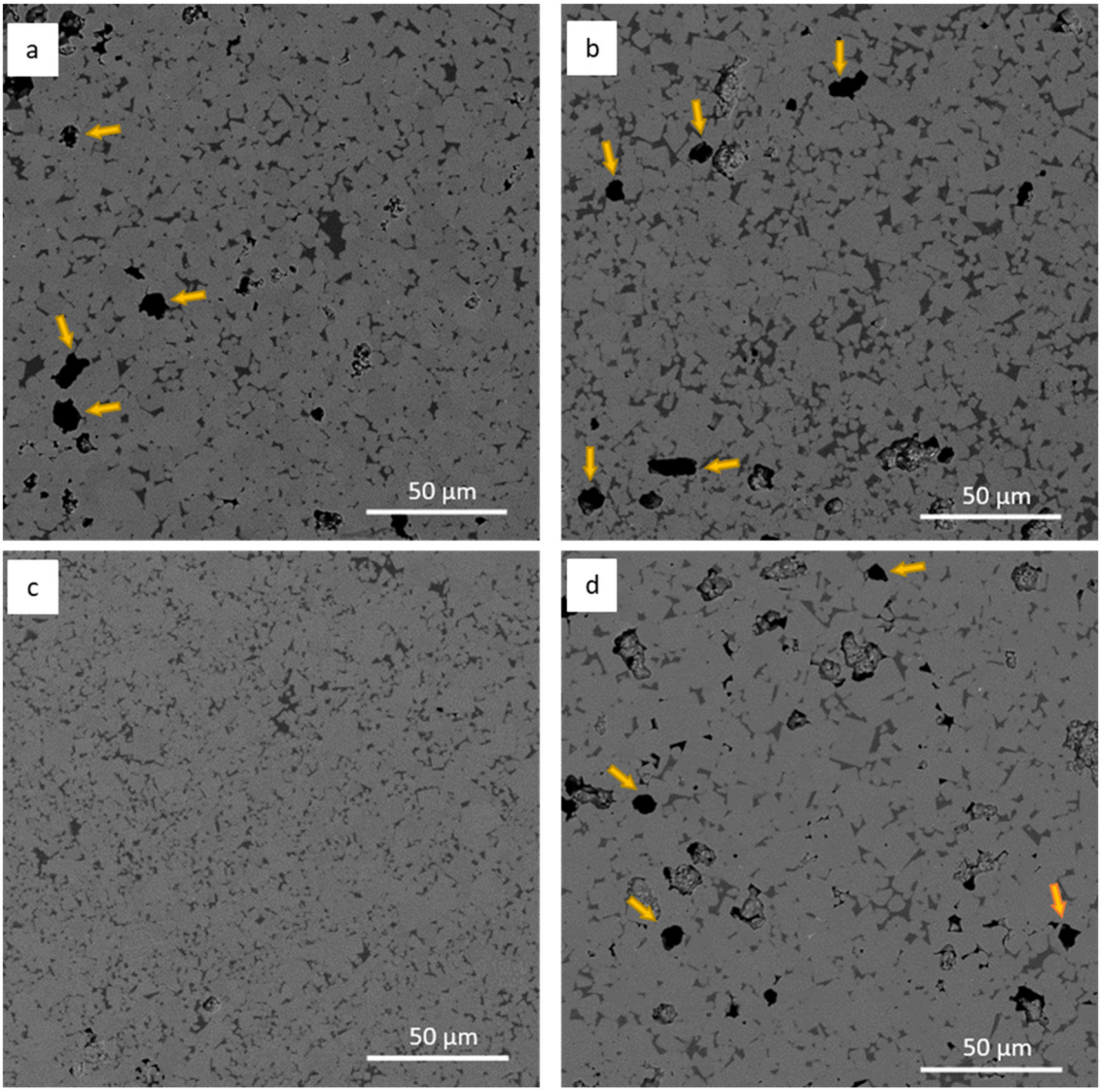

Fig. 2. SEM backscatter micrographs of the sintered NbC-M2 cemented carbide containing (a) 0 wt% (b) 0.1 wt% (c) 0.3 wt%, and (d) 0.9 wt% MWCNTs.

Table 1
Density, relative density and average NbC grain size of the NbC-M2 cemented carbide containing different amounts of MWCNTs after sintering at 1360 °C for 1 h.

MWCNTs (wt%)	0	0.1	0.3	0.9
Density (g.cm^{-3})	7.3136	7.3013	7.5123	7.2893
R.D. (%)	94.50	94.57	97.76	96.20
NbC grain size (µm)	5.54	6.12	7.02	6.87

3.3. Mechanical properties

Vickers hardness and fracture resistance of the sintered NbC-M2-MWCNTs are presented in Fig. 5. The results show that adding small amounts of MWCNTs (i.e., from 0 to 0.3 wt%) increased the hardness from 1101 ± 18 HV to 1470 ± 22 HV, respectively. However, further increase in MWCNTs up to 0.9 wt% caused a drastic drop in hardness down to 997 ± 26 HV. Several factors contribute to the final hardness of cemented carbides. Intrinsic plasticity of ceramic and metallic phases, sintering condition, binder percentage and its distribution, carbide grain size, total carbon content, density, remaining porosities, and bonding strength between the ceramic and metallic phases are the main factors [3,29]. Based on the microstructural investigation (Fig. 2.) and density measurements (Table 1), the high hardness associated with the sample containing 0.3 wt% MWCNTs is mainly due to its higher relative density. Regarding the fracture resistance, a slight variation in its trend can be noted compared to the hardness trend (Fig. 5). The values of fracture resistance do not represent a remarkable change (variation between 2.7 and 3.6 MPa.m$^{0.5}$) when the amount of MWCNTs is increased. A decrease in the fracture resistance is seen after adding 0.1 wt% MWCNTs, followed by an increase to the highest value of 3.55 ± 0.8 MPa.m$^{0.5}$ for the sample containing 0.3 wt% MWCNTs. Finally, a drop in the fracture resistance can be noted when 0.9 wt% MWCNTs are added to the mixtures. There is an optimum value of 0.3 wt% MWCNTs addition to obtain highest fracture resistance value in NbC-M2-MWCNTs cemented carbides. The reduction of fracture resistance by the addition of 0.1 wt% is associated with the formation of undistributed coarse chromium carbide in the binder (Fig. 4.), which has low ductility and leads to weak fracture properties [28]. The ductility of the metal binder mostly influences fracture resistance of the matrix. Moreover, it is shown that coarse carbide grains can accommodate plastic deformation via dislocations, stacking faults, etc. which would affect the fracture resistance as well [30,31]. Considering this fact and the increasing trend of NbC grain size upon addition of MWCNTs shown in Fig. 3., it can be concluded that other toughening mechanisms exist that caused fluctuation in the fracture resistance. In

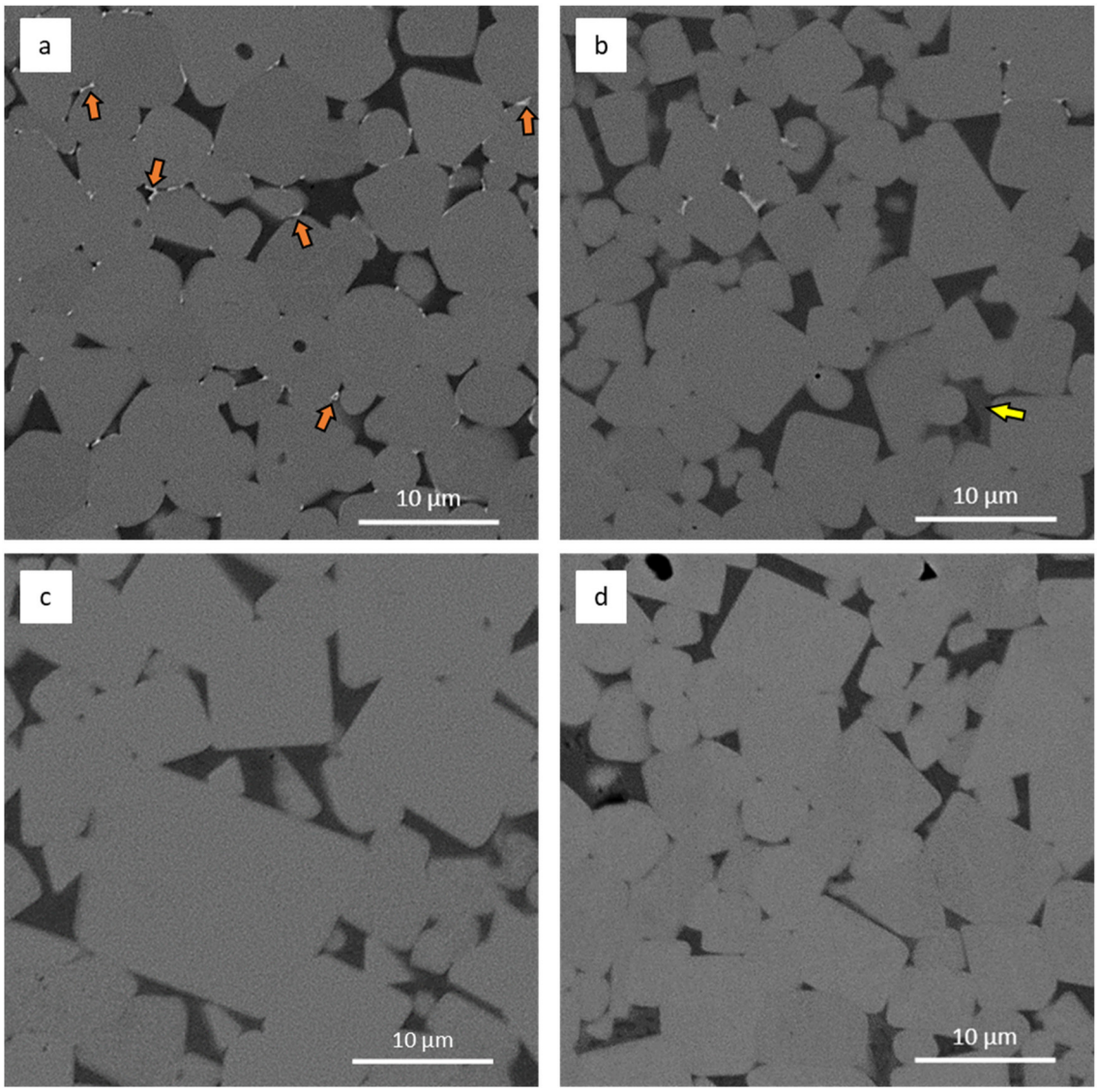

Fig. 3. SEM backscatter images of NbC-M2 containing (a) 0 wt% (b) 0.1 wt% (c) 0.3 wt%, and (d) 0.9 wt% MWCNTs.

order to better understand the mechanisms responsible for enhanced fracture resistance in the sample containing 0.3 wt% MWCNTs, indentation cracks were investigated by SEM. The ability of nanotubes to suppress crack propagation is evident in Fig. 6(a-f). In Fig. 6(b) a bonding between MWCNTs and NbC is evident within the crack. It can be found that the morphology of the NbC is changed into a rod shape at the MWCNTs' tip. According to studies on the formation of metal carbide nanotubes from CNTs and metal powder mixtures [32–34], it is assumed that NbC nanorod is formed at the NbC-MWCNTs interface. Based on Fig. 6(c-f), it seems that the dissipation of crack energy caused by these MWCNTs bridges is responsible for the higher fracture resistance in the NbC-M2-MWCNTs cemented carbides compared to other studies [18]. This toughening mechanism is more active in the NbC-M2–0.3 wt% MWCNTs composite as the highest fracture resistance value was recorded for this sample. Bridging was not observed for the sample containing 0.9 wt% MWCNTs. The lowest hardness and fracture resistance may result from poor dispersion of high MWCNTs loading. It is assumed that imperfect dispersion resulted in heterogeneous stress distribution throughout the cemented carbide. As a result, the existence of high local stress led to the unwanted mechanical properties [35]. This proves that an optimum amount of MWCNTs (here 0.3 wt%) should be added in order to obtain the desired mechanical properties. Similarly, enhancement in mechanical properties of WC-Co cemented carbide was achieved by the addition of 0.3 wt% MWCNTs as well [20].

Considering the mechanical properties of the samples examined in this research, it is clear that the sample containing 0.3 wt% MWCNTs features the superior combination of hardness and fracture resistance. Microstructural analysis confirmed the formation of bridges in the NbC cracks. In order to have a better understanding of the bonding between NbC and MWCNTs, another mixture containing NbC-5 wt% MWCNTs was prepared via the same sintering procedure. The SEM micrograph taken from the fracture surface of this sample is shown in Fig. 7. Some hackle lines could be traced (Fig. 7(a) marked in red). This feature is already reported in a study by Huang et al. [36], which improves fracture resistance of the matrix. Moreover, bridging between NbC grains is observable. The bonding shown in Fig. 7(b) between the grains is not a typical feature of solid-state sintering. Considering MWCNTs' diameter, it is assumed that the MWCNTs have bonded the grains strongly, and an NbC tube is formed around the MWCNTs. This will support the hypothesis of NbC tube formation when being in contact with CNTs [34]. This idea could introduce new approaches in the generation of hybrid metal carbide composites with superior properties.

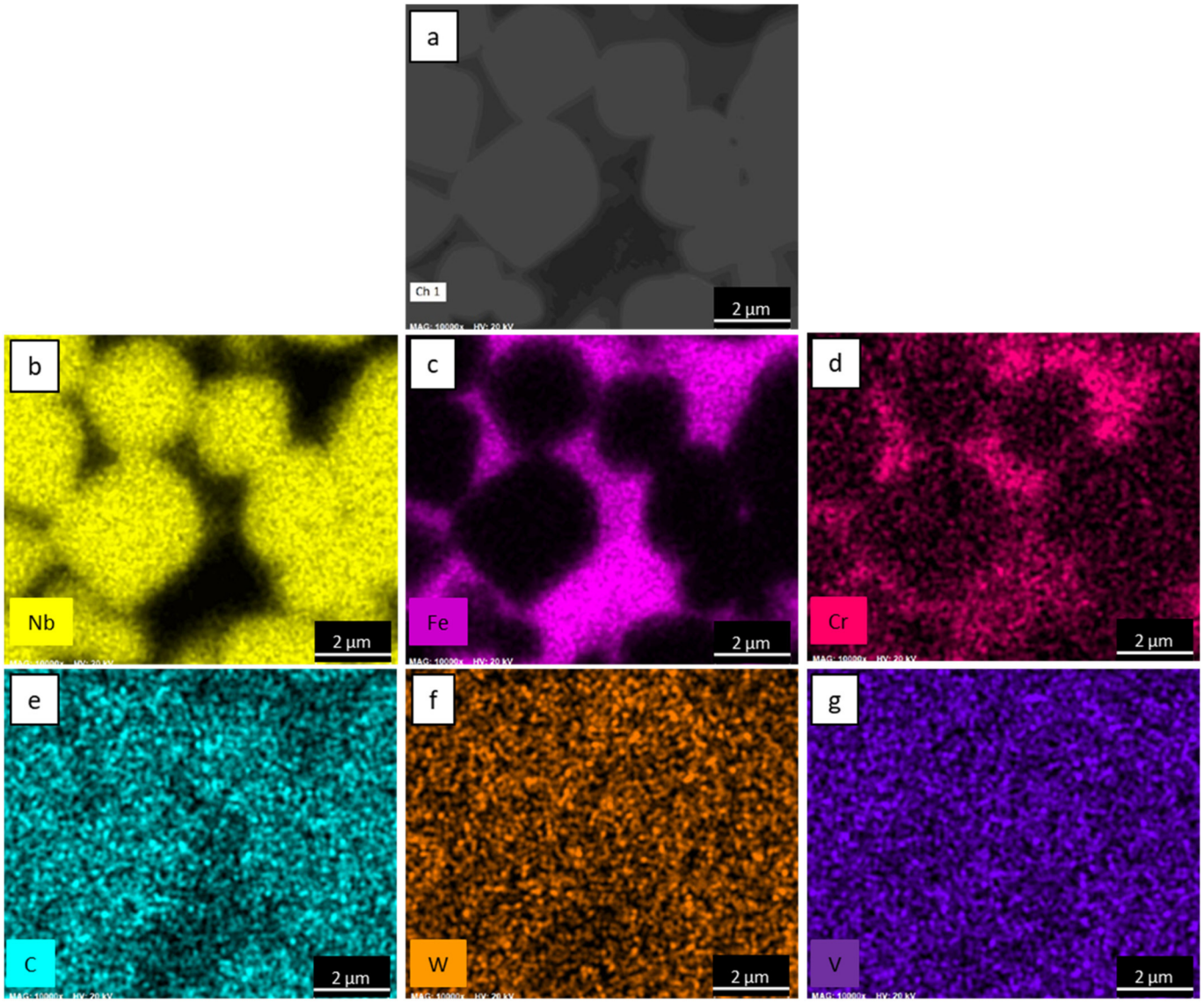

Fig. 4. EDS elemental map of NbC-M2–0.1 wt% MWCNTs sample: (a) SEM micrograph of the selected area for EDS analysis, (b) Nb, (c) Fe, (d) Cr, (e) C, (f) W, and (g) V.

3.4. Phase evolution

Fig. 8. presents X-ray powder diffraction (XRD) patterns of the starting powders. NbC has a B1 cubic rock salt structure with $Fm\bar{3}m$ space group, and its Miller indices are indexed according to JCPDS card number 01–089-3690 (Fig. 8(a)) [37]. M2 steel powder contains two phases, i.e., α-Fe and γ-Fe [38]. Due to high amounts of alloying elements and high cooling rates during gas-atomization, most molten steel has transformed to α-Martensite (JCPDS No. 44–1291). However, a small portion of γ-Fe (JCPDS No. 23–0298) usually exists in the final structure of HSS alloys. Fig. 8(c) shows the XRD pattern of MWCNTs (JCPDS No. 26–1080). The broad peaks represent the nanocrystalline structure of nanotubes [22,39].

The phase evolution of NbC-M2-MWCNTs samples after sintering is shown in Fig. 9(a). From the XRD patterns, two phases i.e., NbC and α-Fe can be identified. As stated in Section 3.2, microstructural analysis via SEM and EDS confirms the presence of three more phases including a white phase containing W, Mo, and Cr (possibly a mixed solid solution carbide) a light grey phase containing Cr, Nb, C (possibly a mixed intermetallic carbide) and MWCNTs. However, these phases are not resolved in XRD patterns, which is due to the limitation of XRD analysis to detect phases below 5 vol% [40]. A magnified view of NbC's first peak is presented in Fig. 9(b). Careful assessment of this peak reveals that a peak shift occurs by introducing MWCNTs from 0 to 0.9 wt% into the structure. A shift towards lower scattering angles means an increase in the lattice parameter [40]. As it was mentioned earlier, MWCNTs addition has changed the solubility of elements in both M2 and NbC phases. It is evident that the high concentration of alloying elements in the NbC structure has caused an expansion of its lattice and thus shifted the scattering angles towards lower values. This behavior confirms the hypothesis of the higher solubility of elements in the NbC structure by increasing MWCNTs loading. Finally, the change in the diffraction angle of the metal binder was not as strong as that of NbC. However, it is proposed that the α-Fe peaks have shifted towards higher angles based on similar research done by Huang et al. [11].

4. Conclusion

Using powder technique, NbC-M2 cemented carbides reinforced with MWCNTs were successfully fabricated. Results show that the addition of 0.3 wt% MWCNTs leads to the desired combination of hardness, relative density, and fracture resistance compared to the samples

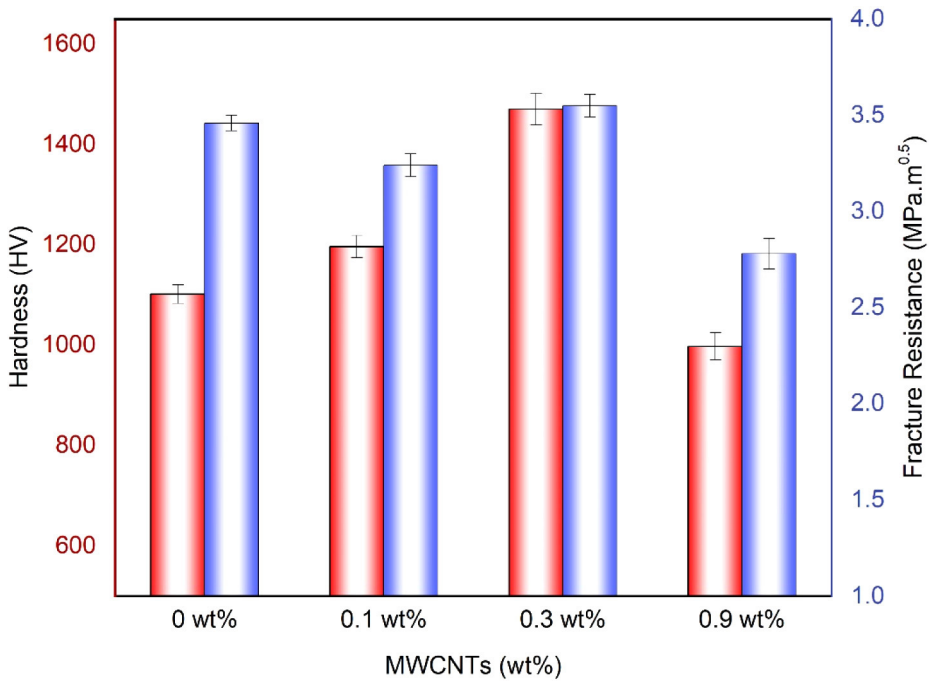

Fig. 5. Vickers hardness and fracture resistance of the sintered NbC-M2 cemented carbide containing different amounts of MWCNTs.

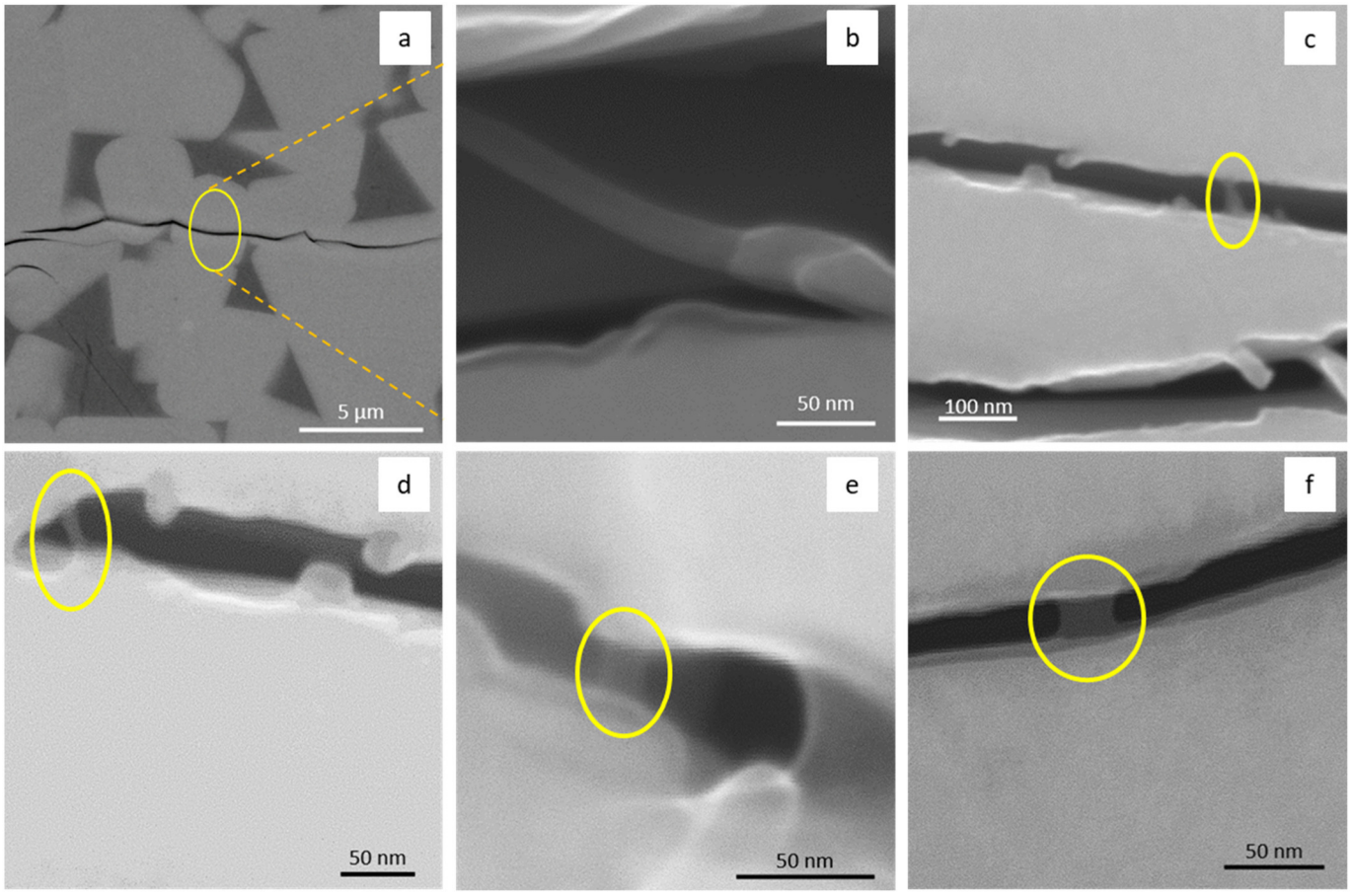

Fig. 6. SEM images of bridging effect of carbon nanotubes formed at the cracks induced by indentation of the sample NbC-M2–0.3 wt% MWCNTs.

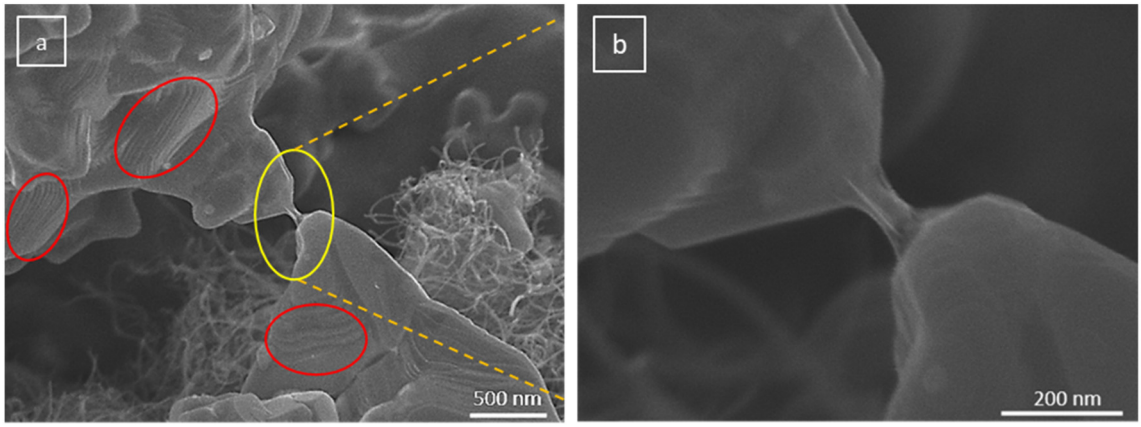

Fig. 7. (a) SEM image of NbC-5 wt% MWCNTs vacuum heated at 1360 °C for 1 h. (b) strong bonding of two NbC grains.

with 0, 0.1, and 0.9 wt% of this material. Maximum hardness, relative density, and fracture resistance of the NbC-M2–0.3 wt% MWCNTs were measured to be 1470 ± 22 HV, 97.76%, and 3.55 ± 0.08 MPa.m$^{0.5}$, respectively.

From the microstructural analysis, it was found that the amount of MWCNTs has a great influence on the appearance of various phases in the microstructure. A mixed carbide phase consisting of W, Mo, and Cr disappears by the addition of MWCNTs. Moreover, EDS analysis confirmed the formation of undistributed coarse carbide phase rich in Cr, Nb, and C in the metal binder. This was observed only in the sample containing 0.1 wt% of MWCNTs. Microstructural investigations demonstrated bridging of MWCNTs in the sample containing 0.3 wt% MWCNTs, which prevented crack propagation, leading to enhanced mechanical properties. Moreover, strong bonding between NbC and MWCNTs was observed, which could be a new approach in reinforcing transition metal carbide composites. X-ray diffraction revealed no major compositional change by adding MWCNTs after sintering. Meanwhile, MWCNTs addition increased the solubility of the alloying elements in the NbC phase resulting in a peak shift in the XRD patterns. It is concluded that incorporating appropriate amounts of carbon nanotubes into the NbC matrix can provide strong bonding between the carbide grains and CNTs and leads to higher fracture resistance.

Author Statement

All persons who meet authorship criteria are listed as authors, and all authors certify that they have participated sufficiently in the work to take public responsibility for the content, including participation in the concept, design, analysis, writing, or revision of the manuscript.

Category 1

Conception and design of study: Cyrus Zamani, A. Hadian, A.M. Hadian, N. Hampp, R. Esmaeilzadeh;

acquisition of data: R. Esmaeilzadeh, H. Reinhardt, M. Dasbach;

analysis and/or interpretation of data: Cyrus Zamani, R. Esmaeilzadeh, A. Hadian, A.M. Hadian, N. Hampp.

Category 2

Drafting the manuscript: R. Esmaeilzadeh, Cyrus Zamani;

revising the manuscript critically for important intellectual content: Cyrus Zamani, R. Esmaeilzadeh, A. Hadian, A.M. Hadian, H. Reinhardt, M. Dasbach;

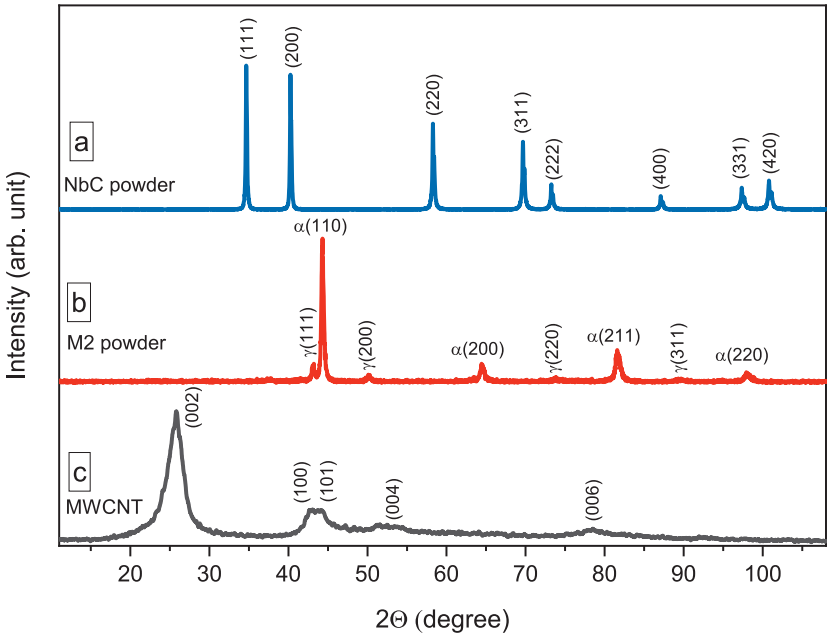

Fig. 8. X-ray diffraction patterns of as-received powders. (a) NbC, (b) M2 high-speed steel, and (c) MWCNTs.

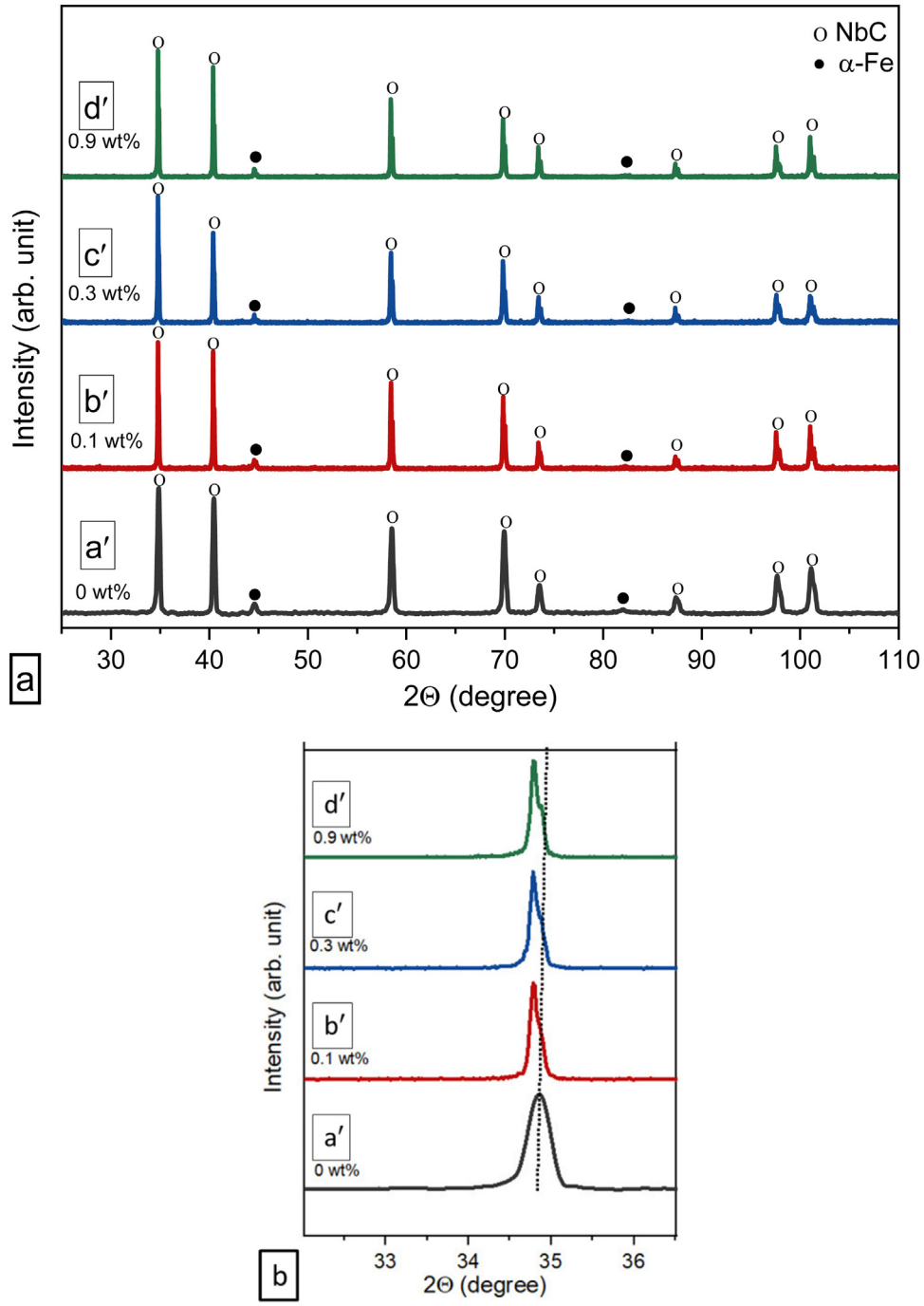

Fig. 9. (a). X-ray diffraction patterns of the sintered NbC-M2 cemented carbide containing MWCNTs. (b) XRD pattern of the highest intensity NbC peak representing a peak shift by adding MWCNTs. (a′) 0 wt%, (b′) 0.1 wt%, (c′) 0.3 wt%, and (d′) 0.9 wt%.

Category 3

Approval of the version of the manuscript to be published: Cyrus Zamani.

Declaration of Competing Interest

The authors declare that they have no known competing financial interests or personal relationships that could have appeared to influence the work reported in this paper.

References

[1] H.O. Pierson, Handbook of Refractory Carbides and Nitrides, Carbides Nitrides, (1996), pp. 100–117, https://doi.org/10.1016/b978-081551392-6.50007-6.
[2] J. García, V. Collado Ciprés, A. Blomqvist, B. Kaplan, Cemented carbide microstructures: a review, Int. J. Refract. Met. Hard Mater. 80 (2019) 40–68, https://doi.org/10.1016/j.ijrmhm.2018.12.004.
[3] V.K. Sarin, Comprehensive Hard Materials, (2014), https://doi.org/10.1016/C2009-1-61070-4.
[4] M. Woydt, H. Mohrbacher, J. Vleugels, S. Huang, Niobium carbide for wear protection – tailoring its properties by processing and stoichiometry, Met. Powder Rep. 71 (2016) 265–272, https://doi.org/10.1016/j.mprp.2015.12.010.
[5] M. Kitaichi, Y. Kitagawa, Hard metal disease, Ryoikibetsu Shokogun Shirizu (1994) 566–568, https://doi.org/10.1136/oem.19.4.239.
[6] T. Kraus, P. Schramel, K.H. Schaller, P. Zöbelein, A. Weber, J. Angerer, Exposure assessment in the hard metal manufacturing industry with special regard to

tungsten and its compounds, Occup. Environ. Med. 58 (2001) 631–634, https://doi.org/10.1136/oem.58.10.631.
[7] S. Bastian, W. Busch, D. Kühnel, A. Springer, T. Meißner, R. Holke, S. Scholz, M. Iwe, W. Pompe, M. Gelinsky, A. Potthoff, V. Richter, C. Ikonomidou, K. Schirmer, Toxicity of tungsten carbide and cobalt-doped tungsten carbide nanoparticles in mammalian cells in vitro, Environ. Health Perspect. 117 (2009) 530–535, https://doi.org/10.1289/ehp.0800121.
[8] M. Woydt, S. Huang, E. Cannizza, J. Vleugels, H. Mohrbacher, Niobium carbide for machining and wear protection – evolution of properties, Met. Powder Rep. 74 (2019) 82–89, https://doi.org/10.1016/j.mprp.2019.02.002.
[9] S.G. Huang, J. Vleugels, H. Mohrbacher, Stainless steel bonded NbC matrix cermets using a submicron NbC starting powder, Int. J. Refract. Met. Hard Mater. 63 (2017) 26–31, https://doi.org/10.1016/j.ijrmhm.2016.04.021.
[10] R.M. Genga, L.A. Cornish, M. Woydt, A. Janse van Vuuren, C. Polese, Microstructure, mechanical and machining properties of LPS and SPS NbC cemented carbides for face-milling of grey cast iron, Int. J. Refract. Met. Hard Mater. 73 (2018) 111–120, https://doi.org/10.1016/j.ijrmhm.2017.12.036.
[11] S. Huang, P. De Baets, J. Sukumaran, H. Mohrbacher, M. Woydt, J. Vleugels, Effect of carbon content on the microstructure and mechanical properties of NbC-Ni based cermets, Metals (Basel). 8 (2018) 1–13, https://doi.org/10.3390/met8030178.
[12] A. Hadian, C. Zamani, F.J. Clemens, Effect of sintering temperature on microstructural evolution of M48 high speed tool steel bonded NbC matrix cemented carbides sintered in inert atmosphere, Int. J. Refract. Met. Hard Mater. 74 (2018) 20–27, https://doi.org/10.1016/j.ijrmhm.2018.02.021.
[13] A. Hadian, C. Zamani, F.J. Clemens, Sintering behavior of NbC based cemented carbides bonded with M2 high speed steel, Ceram. Int. 45 (2019) 8616–8625, https://doi.org/10.1016/j.ceramint.2019.01.181.
[14] A. Hadian, C. Zamani, L. Gorjan, F.J. Clemens, Thermoplastic processing and debinding behavior of NbC-M2 high speed steel cemented carbide, J. Mater. Process. Technol. 263 (2019) 91–100, https://doi.org/10.1016/j.jmatprotec.2018.08.006.
[15] S.G. Huang, J. Vleugels, H. Mohrbacher, M. Woydt, NbC grain growth control and mechanical properties of Ni bonded NbC cermets prepared by vacuum liquid phase sintering, Int. J. Refract. Met. Hard Mater. 72 (2018) 63–70, https://doi.org/10.1016/j.ijrmhm.2017.12.013.
[16] S.G. Huang, J. Vleugels, H. Mohrbacher, M. Woydt, Microstructure and mechanical properties of NbC matrix cermets using Ni containing metal binder, Met. Powder Rep. 71 (2016) 349–355, https://doi.org/10.1016/j.mprp.2016.05.009.
[17] S.G. Huang, H.B. Nie, X.Y. Guo, J. Vleugels, J.H. Huang, H. Mohrbacher, N.K. Rajendhran, J. Sukumaran, P. De Baets, E. Cannizza, M. Woydt, Microstructural investigation and machining performance of NbC-ti(C0.5N0.5) matrix cermets, Int. J. Refract. Met. Hard Mater. 84 (2019) 105038, , https://doi.org/10.1016/j.ijrmhm.2019.105038.
[18] J. Cho, A.R. Boccaccini, M.S.P. Shaffer, Ceramic matrix composites containing carbon nanotubes, J. Mater. Sci. 44 (2009) 1934–1951, https://doi.org/10.1007/s10853-009-3262-9.
[19] Z. Xia, L. Riester, W.A. Curtin, H. Li, B.W. Sheldon, J. Liang, B. Chang, J.M. Xu, Direct observation of toughening mechanisms in carbon nanotube ceramic matrix composites, Acta Mater. 52 (2004) 931–944, https://doi.org/10.1016/j.actamat.2003.10.050.
[20] F. Zhang, J. Shen, J. Sun, Processing and properties of carbon nanotubes-nano-WC-co composites, Mater. Sci. Eng. A 381 (2004) 86–91, https://doi.org/10.1016/j.msea.2004.03.061.
[21] D.K. Shetty, I.G. Wright, P.N. Mincer, A.H. Clauer, Indentation fracture of WC-co cermets, J. Mater. Sci. 20 (1985) 1873–1882, https://doi.org/10.1007/BF00555296.
[22] T. Belin, F. Epron, Characterization methods of carbon nanotubes: a review, Mater. Sci. Eng. B Solid-State Mater. Adv. Technol. 119 (2005) 105–118, https://doi.org/10.1016/j.mseb.2005.02.046.
[23] J.H. Lehman, M. Terrones, V. Meunier, E. Mansfield, K.E. Hurst, Evaluating the characteristics of multiwall carbon, Carbon N. Y. 49 (2011) 2581–2602, https://doi.org/10.1016/j.carbon.2011.03.028.
[24] H. Andren, Microstructures of cemented carbides, Mater. Des. (2001) 491–498, https://doi.org/10.1016/S0261-3069(01)00006-1.
[25] X.L. Shi, H. Yang, S. Wang, G. Shao, X. Duan, Fabrication and properties of WC-10Co cemented carbide reinforced by multi-walled carbon nanotubes, Mater. Sci. Eng. A 486 (2008) 489–495, https://doi.org/10.1016/j.msea.2007.10.022.
[26] R.M. German, Liquid Phase Sintering, Springer Science + Business Media, New York, 1985, https://doi.org/10.1007/978-1-4899-3599-1.
[27] Q. Yang, S. Yu, C. Zheng, J. Liao, J. Li, L. Chen, S. Guo, Y. Ye, H. Chen, Effect of carbon content on microstructure and mechanical properties of WC-10Co cemented carbides with plate-like WC grain, Ceram. Int. (2019) 1824–1829, https://doi.org/10.1016/j.ceramint.2019.09.158.
[28] M.G. di V. Cuppari, S.F. Santos, Physical properties of the NbC carbide, Metals (Basel) 6 (2016), https://doi.org/10.3390/met6100250.
[29] X. Zhao, M. Togaru, Q. Guo, C.R. Weinberger, L. Lamberson, G.B. Thompson, Carbon influence on fracture toughness of niobium carbides, J. Eur. Ceram. Soc. 39 (2019) 5167–5173, https://doi.org/10.1016/j.jeurceramsoc.2019.08.022.
[30] X. Liu, J. Zhang, C. Hou, H. Wang, X. Song, Z. Nie, Mechanisms of WC plastic deformation in cemented carbide, Mater. Des. 150 (2018) 154–164, https://doi.org/10.1016/j.matdes.2018.04.025.
[31] G. Östberg, K. Buss, M. Christensen, S. Norgren, H.O. Andrén, D. Mari, G. Wahnström, I. Reineck, Mechanisms of plastic deformation of WC-co and ti(C, N)-WC-co, Int. J. Refract. Met. Hard Mater. 24 (2006) 135–144, https://doi.org/10.1016/j.ijrmhm.2005.04.009.
[32] E.W. Wong, B.W. Maynor, L.D. Burns, C.M. Lieber, Growth of metal carbide nanotubes and nanorods, Chem. Mater. 4756 (1996) 2041–2046, https://doi.org/10.1021/cm960083b.
[33] K. Kobayashi, R. Kitaura, Q. Wang, I. Wakamori, H. Shinohara, S. Anada, T. Nagase, T. Saito, M. Kiyomiya, H. Yasuda, Synthesis of refractory conductive niobium carbide nanowires within the inner space of carbon nanotube templates, Appl. Phys. Express 7 (015101) (2014) 5–9, https://doi.org/10.7567/APEX.7.015101.
[34] Y. Zhang, Heterostructures of single-walled carbon nanotubes and carbide nanorods, Science 285 (5434) (1999) 1719–1722, https://doi.org/10.1126/science.285.5434.1719.
[35] P. Kenny, The application of fracture mechanics to cemented tungsten carbide, Powder Metall. 14 (1971) 22–38, https://doi.org/10.1179/pom.1971.14.27.002.
[36] S.G. Huang, J. Vleugels, H. Mohrbacher, M. Woydt, Microstructure and tribological performance of NbC-Ni cermets modified by VC and Mo2C, Int. J. Refract. Met. Hard Mater. 66 (2017) 188–197.
[37] C.J. Smith, C.R. Weinberger, G.B. Thompson, Phase stability and microstructural formations in the niobium carbides, J. Eur. Ceram. Soc. 38 (2018) 4850–4866, https://doi.org/10.1016/j.jeurceramsoc.2018.06.041.
[38] I.H. Sharma, S. Sharma, Cryogenic processing of HSS M2: mechanical properties and XRD analysis, MATEC Web Conf. 57 (2016), https://doi.org/10.1051/matecconf/20165703009.
[39] W.H. Tan, S.L. Lee, C.T. Chong, TEM and XRD analysis of carbon nanotubes synthesised from flame, Key Eng. Mater. (2017) 470–475, https://doi.org/10.4028/www.scientific.net/KEM.723.470 723 KEM.
[40] B.D. Cullity, S.R. Stock, Elements of X-Ray Diffraction, 3rd ed, Pearson Education Limited, 2014.